

Building the Stellar Halo Through Feedback in Dwarf Galaxies

Aaron J. Maxwell, James Wadsley, H. M. P. Couchman, & Sergey Mashchenko

*Department of Physics & Astronomy, McMaster University, Hamilton, ON, L8S 4M1,
CAN*

ajmax@mcmaster.ca

ABSTRACT

We present a new model for the formation of stellar halos in dwarf galaxies. We demonstrate that the stars and star clusters that form naturally in the inner regions of dwarfs are expected to migrate from the gas rich, star forming centre to join the stellar spheroid. For dwarf galaxies, this process could be the dominant source of halo stars. The effect is caused by stellar feedback-driven bulk motions of dense gas which, by causing potential fluctuations in the inner regions of the halo, couple to all collisionless components. This effect has been demonstrated to generate cores in otherwise cuspy cold dark matter profiles and is particularly effective in dwarf galaxy haloes. It can build a stellar spheroid with larger ages and lower metallicities at greater radii without requiring an outside-in formation model. Globular cluster-type star clusters can be created in the galactic ISM and then migrate to the spheroid on 100 Myr timescales. Once outside the inner regions they are less susceptible to tidal disruption and are thus long lived; clusters on wider orbits may be easily unbound from the dwarf to join the halo of a larger galaxy during a merger. A simulated dwarf galaxy ($M_{\text{vir}} \simeq 10^9 M_{\odot}$ at $z = 5$) is used to examine this gravitational coupling to dark matter and stars.

Subject headings: galaxies: dwarf — galaxies: evolution — galaxies: formation — galaxies: star clusters: general

1. Introduction

Dwarf galaxies are the predominant star forming objects in the early universe and dwarf spheroidals, in particular, are fossil remnants of this era (Dekel & Silk 1986). Normal star formation (post-Population III) occurs in the densest gas accumulating in the centres of galactic potential wells. In this case, we might expect dwarf spheroids to be simple, highly concentrated, star piles. In contrast, the stars in observed dwarfs are diffuse and many lack

a conspicuous nucleus. Further, dwarfs at or above the luminosity of Fornax have their own globular cluster systems (Mateo 1998). If these galaxies were the first objects large enough to have a high-pressure ISM in their centres, capable of forming large clusters, we need to explain how such clusters could end up orbiting at substantial radii with a distribution similar to that of the overall light (Miller 2009). Radial age and metallicity gradients are also observed (McConnachie 2012), suggesting an outside-in formation scenario reminiscent of the “monolithic collapse” model (Eggen et al. 1962, hereafter ELS).

In this paper, we explore how features present in the old stellar populations of dwarf galaxies can occur naturally in contemporary cosmological models through star formation and feedback in these galaxies. Young dwarf galaxies have a high gas content and form stars vigorously. In prior work, Mashchenko et al. (2008) were able to show that stellar feedback in a simulated dwarf galaxy will drive bulk gas motions that couple gravitationally to all matter near the centre of the dwarf. As discussed in §2, this mechanism has been shown to act in actively star forming galaxies at a range of masses and is believed to be generic. The process pumps energy into the orbits of all material passing near the centre, transforming an initial dark matter cusp into a broad core, consistent with observations. Here we study the evolution of the stellar content, which is formed self-consistently in those simulations. Orbit pumping also operates on stars, the other key collisionless component of galaxies, to grow stellar spheroids from the inside out, as well as place massive star clusters on large radial orbits.

It is widely understood that the Λ CDM cosmology predicts the hierarchical assembly of galaxies: dwarf proto-galaxies interact and merge into larger galaxies, contrary to the ELS model. Searle & Zinn (1978) and Zinn (1980) refined this model by invoking a late in-fall of old stars that would contribute to both the stellar halo and its globular cluster population. Subsequent work has focused on reconciling this picture for the formation of the Galactic stellar halo with the standard hierarchical framework (for a recent review see Helmi 2008). Chemical enrichment models combined with descriptions of a Milky Way (MW)-type merger history (e.g. Robertson et al. 2005; Bullock & Johnston 2005; De Lucia & Helmi 2008) and cosmological simulations of MW-type galaxies (e.g. Zolotov et al. 2010) can be made to match the abundance patterns of the stellar halo (e.g. Carollo et al. 2007, 2010; de Jong et al. 2010). A general conclusion is that dwarf progenitors play a major role in building the MW halo, owing to their high rates of star formation at early times and their ability to retain supernova-enriched gas.

However, MW-scale simulations poorly resolve dwarf galaxies which thus readily disintegrate and contribute their entire stellar contents to the halo. This conclusion is a direct consequence of low numerical resolution and is at odds with how star formation would be expected to occur in dwarfs. A closer understanding of star formation in dwarf galaxies is needed to establish how those stars are produced and how readily they can contribute to the

observed Galactic stellar populations and their radial variations.

In §2 we discuss the stellar redistribution mechanism and how it operates. In §3 we explore the impact this has on the formation of the stellar spheroid in dwarfs including stellar systems such as globular clusters. We also discuss implications for dwarfs contributing their stars to the spheroids of larger galaxies.

2. Dynamical Impact of Stellar Feedback

Observations of the kinematics of the stellar and gaseous components of dwarf galaxies point to these systems having a cored density profile (e.g. Burkert 1995; Côté et al. 2000; Gilmore et al. 2007; Oh et al. 2011, see de Blok (2010) for a recent review) in contrast to collisionless simulations of Cold Dark Matter (CDM) haloes which predict a central density cusp (e.g. Dubinski & Carlberg 1991; Navarro et al. 1995; Bullock et al. 2001; Klypin et al. 2001; Stadel et al. 2009). Mashchenko et al. (2008) presented a solution to this long-standing challenge for the CDM cosmogony by correctly accounting for the the impact of stellar feedback. By feeding the energy generated by supernovae into the surrounding star-forming gas, they were able to generate fluctuations in the gravitational potential that pumped the dark matter orbits and removed the cusp. The effectiveness of dark matter orbit pumping due to stellar feedback has been confirmed in simulations by other workers, showing that it operates in dwarfs to the present day (Governato et al. 2010) and also affects larger galaxies up to Milky Way scales with sufficiently strong feedback (Macciò et al. 2012). In addition to operating in the SPH code used by Mashchenko et al. (2008), the mechanism has also been demonstrated using a grid code¹.

Two critical features allowed Mashchenko et al. (2008) to demonstrate the effect of stellar feedback on dark matter orbits in the dwarf galaxy: high resolution ($300 M_{\odot}$ per gas particle) and low temperature metal cooling (10–8000 K). The combination of these features allowed the formation of a cold, dense gas phase and permitted the use of a far more realistic minimum density for star formation, $\sim 100 \text{ atoms cm}^{-3}$, comparable to molecular cloud densities. This was in sharp contrast to prior work where star formation occurred fairly uniformly throughout the ISM of simulated galaxies. As a result this was the first cosmological simulation to form numerically resolved star clusters up to $\sim 10^5 M_{\odot}$.

A direct result of clustered star formation is highly localized and episodic feedback that violently rearranges the gas in the inner regions of the dwarf galaxy. Since the gas dominates the mass in the star forming region, this results in a gravitational potential that varies on a timescale commensurate with orbital times. This causes irreversible changes in the

¹R. Teyssier, priv. comm.

orbital energies of all matter passing near the star-forming centre of the dwarf. Whereas sharp changes in the potential impulsively modify all particle orbits (Pontzen & Governato 2012), Mashchenko et al. (2006) showed that oscillating potentials with speeds closer to the typical particle velocity couple strongly and flatten the core more rapidly (their figure 2). For material that initially has a low velocity dispersion, such as dark matter within the cusp, this preferentially increases the orbital radius and redistributes the material into a smooth core as shown in Mashchenko et al. (2008) and other works. For the gaseous component, shocks dissipate this added velocity whereas dark matter and stars undergo a random walk in orbital energy.

We use the simulated dwarf of Mashchenko et al. (2008) to illustrate the process. We selected a period between redshifts 8–5 without major mergers so that the evolution is dominated by centralized star formation fueled by a consistent gas supply. Figure 1 shows several cycles of star formation, feedback upon the gas content and the response of the collisionless components. In this simulation, the majority of stars form within 100 pc, which we use as a radial size in which to measure the feedback effects. The centre is defined as the position of the 100 most bound particles. This choice biases towards gas-rich star-forming regions but gives very similar results to using a mass-weighted centre. The central 100 pc region is well resolved in space and mass.

In Figure 1a, the total star formation rate in units of $M_{\odot} \text{yr}^{-1}$ is shown for all stars formed within 100 pc. The star formation is highly episodic in this redshift range. Given that star formation is confined to a small central region, stellar feedback is very efficient at cutting off the supply of cold, dense gas that fuels the process. In the feedback model employed in this simulation, the effective component is supernova energy injection acting over a period of 10–30 Myr after initial star formation. Thus, once initiated within a dense knot of gas, star formation rises to a peak and shuts down in around 10 Myr. The five highest peaks in the central star formation rate are marked with vertical dotted lines to guide the eye over the four panels of the figure.

The solid line in Figure 1b shows the enclosed gas mass in units of M_{\odot} as a function of time within 100 pc. The enclosed gas mass shows the same cyclic behaviour as the star formation rate with a lag of 10–20 Myr. Gas falls into the inner regions, forming dense clouds and allowing star formation to begin. Stellar feedback starts to pressurize the gas leading to both compression and the driving of material out of the inner regions. The gas velocity dispersion varies from $10\text{--}40 \text{ km s}^{-1}$ within 100 pc, indicating crossing times of roughly 5–20 Myr. Thus the gas mass peaks slightly after the peak in star formation and then subsides.

The total gas mass (triple-dot-dash line in the same panel) within 3.2 kpc (the virial radius at $z = 8$) increases steadily due to fresh in-falling material, reaching $\sim 2 \times 10^8 M_{\odot}$ at $z = 5$. Feedback associated with vigorous star formation can readily create hot gas ($T > 10^6 \text{ K}$) and outflows exceeding the 100 km s^{-1} escape velocity. Such unbound gas can

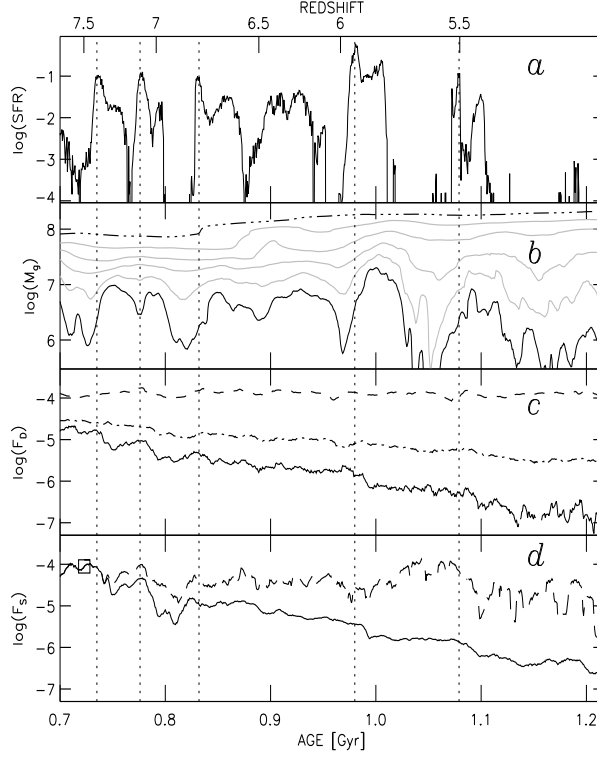


Fig. 1.— Star formation rate, variation of enclosed gas mass and variation of phase-space density for the collisionless components.

a) Star formation rate ($M_\odot \text{ yr}^{-1}$) within a radius of 100 pc of the centre. Vertical dotted lines highlight 5 strong star formation peaks.

b) Enclosed gas mass (M_\odot) for various radii. The solid line is for a 100 pc radius, and the grey lines increase the radius by a factor of two each step. The triple-dot-dash line is the enclosed mass within 3.2 kpc.

c) The dark matter phase-space density ($M_\odot \text{ pc}^{-3} \text{ km}^{-3} \text{ s}^3$) measured within 100 pc. The solid line indicates low velocity dark matter (see text) while the dash-dot is for all dark matter. The dashed line shows the behaviour in a simulation without stellar feedback.

d) The stellar phase-space density ($M_\odot \text{ pc}^{-3} \text{ km}^{-3} \text{ s}^3$) measured within 100 pc. The solid line is for stars formed before $z = 7.5$ (time stamp denoted by the square), while the long-dash line is for all stars.

travel tens of kiloparsecs from the dwarf. However, the total mass in unbound (mostly hot) gas generated is comparable to the $3 \times 10^7 M_\odot$ in stars created over the 500 Myr period shown in Figure 1. In-fall onto the galaxy continues steadily along cold filaments next to the outflow channels and is not disrupted by the outflow, as the figure indicates. The baryon fraction inside the virial radius is always moderately in excess of the universal baryon fraction. The gas mass within the star forming inner region fluctuates dramatically in response to feedback but much of this gas is simply cycling within the inner few hundred parsecs. Within 800 pc the gas content grows fairly smoothly as shown by the second-to-top grey curve.

The numerical values for star formation rates and mass outflows are a result of the specific sub-grid models and resolution used for this simulation (though the resolution is much higher than is typical). However, the qualitative picture is expected to be robust and is consistent with our understanding of feedback and its role in creating a bursty star formation history in smaller galaxies (Stinson et al. 2007). The gas within the entire halo is characterized by churning motions with colder gas moving in and hotter gas moving out. This is in contrast to the simple gas blow-out picture of the evolution of dwarf galaxies (e.g. Navarro et al. 1996) where the entire star-forming gas content is at least temporarily evacuated. The advantage here is the continual availability of gas for ongoing star formation with bursts on the dynamical timescale of the dense inner regions (50–100 Myr) that repeatedly perturb the collisionless components. This type of churning also occurs in more massive galaxies (Brook et al. 2012).

Figure 1c shows the behaviour of the central dark matter phase-space density, approximated as ρ/σ^3 , where ρ is the mean dark matter density and σ is the velocity dispersion within the central 100 pc. Whereas the fine-grained, dark matter, 6-dimensional phase-space density is strictly conserved, the coarse-grained dark matter phase-space density, which we are approximating with ρ/σ^3 , is insensitive to adiabatic compression due to baryonic dissipation but should decrease monotonically due to irreversible (non-adiabatic) effects.

The dot-dash line is for all dark matter particles located within 100 pc of the centre at each simulation output. The solid line shows the behaviour of a group of dark matter particles with velocities less than 20 km s^{-1} , selected at $z = 8$, and followed throughout the simulation. Both dark matter groups show a steady decrease in the coarse-grained phase-space density 10–20 Myr after a star formation peak. Note, however, that the low velocity dark matter exhibit much steeper gradients. This decrease is associated with both an increase in their velocity dispersion and a decrease in their density. This persistent decrease of ρ/σ^3 , unaffected by the gas returning to the core, demonstrates that the heating of collisionless matter through the gas-driven gravitational potential oscillations is irreversible. The long term effect is a random walk in orbital energy that redistributes dark matter particles into a cored profile of order 400 pc in size by $z = 5$ as shown by Mashchenko et al. (2008). In the same dwarf simulated without any star formation, the phase-space density remains

relatively constant as shown by the dashed line.

3. Stars: The Other Collisionless Component

Stars also behave as a collisionless fluid, and so couple to the potential fluctuations created by stellar-feedback-driven gas motions. Indeed, the majority of stars are formed within the dwarf core and spread outwards by the end of the simulation. The central stellar density is regularly increased by new stars which are then dispersed to larger orbits. The long-dash line in Figure 1d shows the phase-space density for all stars within 100 pc. As the stellar density within this radius is replenished by star formation, there is no significant trend in the phase-space density. To examine the evolution of stars after their formation, we selected stars within the inner 100 pc that were formed before 0.72 Gyr and tracked their phase-space density over time as indicated by the solid line. The decrease in phase-space density is dramatic, comparable to that for the low-velocity-dispersion dark matter. Since the stars form from gas with velocity dispersion $\sim 20 \text{ km s}^{-1}$, these trends reflect the greater efficiency of this heating mechanism for low velocity material. Note also that significant decreases in the phase-space density occur 10–20 Myr after the central bursts of star formation, as discussed above. In our simulated dwarf, stellar orbits are found to expand to beyond 1 kpc through the effects of this mechanism.

3.1. The Diffuse Spheroid

In this new picture, stars form preferentially in spatially concentrated star bursts near the gas-rich centres of small galaxies and then migrate to the outer parts of the galaxy. Orbital changes occur repeatedly for objects traversing the star forming core. This effect will not be limited to small galaxies but may become less pronounced for larger halos. The degree to which stars have migrated is a function of their time of formation and the period of time for which sufficiently vigorous potential fluctuations were available to pump their orbits. This provides an alternative to simply scaling the ELS view down to smaller halo masses.

Figure 2 shows that even though half the stars formed inside 100 pc (solid line), by the end of the simulation (500 Myr later) they fill the entire dwarf halo with no distinction between those that formed inside and outside 100 pc. New stars take time to move outward and when star formation stops, so does the orbital expansion. The result at $z = 5$ is a moderate trend to larger stellar ages with radius. This may explain the age and metallicity gradients believed to be present in the Local Group Dwarfs (Mateo 1998).

3.2. Bound Star Clusters

As noted above, the star formation that occurs in the simulation is clustered in character due to the unusually high spatial resolution ($100 M_{\odot}$ per star particle) and modeling of low temperature cooling (Mashchenko et al. 2008), consistent with the majority of star formation in nature. The majority of these clusters are disrupted as the simulation progresses, and the stars are deposited across the stellar spheroid of the dwarf. This is partly a resolution effect as the gravitational resolution of the simulation (10 pc) will not result in smaller, more tightly bound clusters. There are, however, a few of these clusters that survived for at least 200 Myr. The four most massive and well resolved clusters (100–1000 stellar particles) were identified within the dwarf spheroid near the end of the simulation and their orbits traced backwards to the point at which 10% of the stars within each cluster had formed. The radial component of the orbits for the four clusters are shown in Figure 3. These four massive clusters form well within 100 pc but are then driven out to large radii as each pericentric passage brings them close to the actively star-forming galactic centre. The process is a random walk with an average tendency to increase the apocentric distance. These clusters also show changes in the direction and magnitude of their orbital angular momenta. The process should be less effective for higher orbital velocities and is thus expected to saturate when the orbits are well outside the star forming region.

Our approach to the building of dwarf spheroids may shed light on the formation of Globular Clusters. Since the same mechanism migrates both stars and stellar clusters to the diffuse spheroid, it provides a natural explanation for the radial distribution seen in dwarf galaxies outside the Local Group (e.g. Miller 2009). Furthermore, the time that the clusters are resident in the inner star forming region (which has grown to ~ 300 pc by $z = 5$) is typically at least 10^8 yr. Visual inspection of the simulation indicates that dense gas knots move with the clusters during this period, thus providing a simple explanation for the recently observed multiple generations of stars within globular clusters (e.g. D’Ercole et al. 2010).

4. Conclusions

We have presented a new framework for understanding the formation of the stellar spheroid in dwarf galaxies: All stars form in the nuclear regions and are then redistributed to eventually occupy the entire halo. The redistribution mechanism relies on strong fluctuations in the baryon-dominated central gravitational potential that are associated with stellar feedback as first demonstrated by Mashchenko et al. (2008). These fluctuations irreversibly affect the orbits and hence distributions of the collisionless components: dark matter, stars

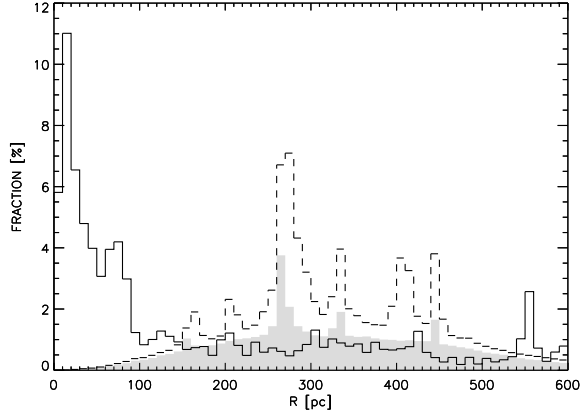


Fig. 2.— The normalized distribution of stellar formation radius (solid) and the final stellar radius (dashed). The shaded region corresponds to the distribution of final radii for the stars that formed within 100 pc.

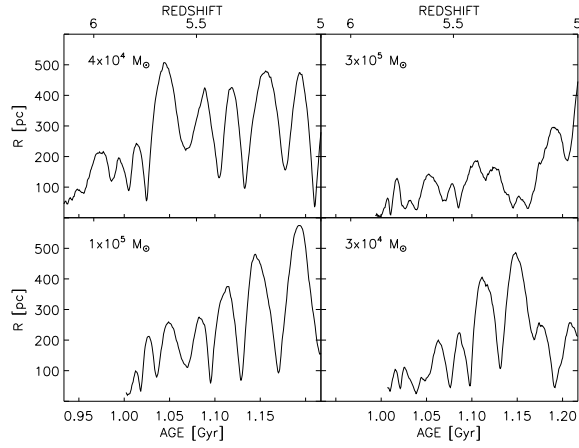


Fig. 3.— Evolution of orbital radii for four long-lived star clusters in the simulation.

and star clusters. The key implications are:

- This process directly affects dwarf galaxies. In these galaxies a mild gradient with radius of increasing age and decreasing metallicity would be created as older stars achieve the largest orbits. Orbital redistribution stops when vigorous star formation ceases.
- The central density of stars stays fairly constant as new stars form to replace those migrating outwards.
- Globular cluster-like star clusters form in the ISM (and thus have no associated dark matter) and migrate outward over several orbital periods.
- The star clusters may form multiple generations of stars from enriched gas readily available in the nuclear regions. They will lose access to new gas as their orbits become larger.
- Continuous creation and outward migration of stars and globular clusters avoids the formation of a super-nucleus at the centre of most dwarf galaxies.
- Larger clusters become protected against tidal destruction as their orbits grow and the dwarf’s dark-matter core becomes flattened.
- Mergers and tidal stripping will deposit these loosely bound stars and clusters into the halo of later generations of larger galaxies.
- Large star clusters formed in dwarf galaxies at high redshift, rather than in dark matter mini-halos, could be the primary source of Globular Clusters in all galaxies.

This work has made use of the SHARCNET Consortium, part of the Compute/Calcul Canada Network. AJM, HMPC and JWW are recipients of NSERC funding. HMPC acknowledges support from CIFAR.

REFERENCES

- Brook, C. B., Stinson, G., Gibson, B. K., et al. 2012, MNRAS, 419, 771
- Bullock, J. S. & Johnston, K. V. 2005, ApJ, 635, 931
- Bullock, J. S., Kolatt, T. S., Sigad, Y., et al. 2001, MNRAS, 321, 559
- Burkert, A. 1995, ApJ, 447, L25
- Carollo, D., Beers, T. C., Chiba, M., et al. 2010, ApJ, 712, 692

- Carollo, D., Beers, T. C., Lee, Y. S., et al. 2007, *Nature*, 450, 1020
- Côté, S., Carignan, C., & Freeman, K. C. 2000, *AJ*, 120, 3027
- de Blok, W. J. G. 2010, *Advances in Astronomy*, 2010
- de Jong, J. T. A., Yanny, B., Rix, H.-W., et al. 2010, *ApJ*, 714, 663
- De Lucia, G. & Helmi, A. 2008, *MNRAS*, 391, 14
- Dekel, A. & Silk, J. 1986, *ApJ*, 303, 39
- D’Ercole, A., D’Antona, F., Ventura, P., Vesperini, E., & McMillan, S. L. W. 2010, *MNRAS*, 407, 854
- Dubinski, J. & Carlberg, R. G. 1991, *ApJ*, 378, 496
- Eggen, O. J., Lynden-Bell, D., & Sandage, A. R. 1962, *ApJ*, 136, 748
- Gilmore, G., Wilkinson, M. I., Wyse, R. F. G., et al. 2007, *ApJ*, 663, 948
- Governato, F., Brook, C., Mayer, L., et al. 2010, *Nature*, 463, 203
- Helmi, A. 2008, *A&A Rev.*, 15, 145
- Klypin, A., Kravtsov, A. V., Bullock, J. S., & Primack, J. R. 2001, *ApJ*, 554, 903
- Macciò, A. V., Stinson, G., Brook, C. B., et al. 2012, *ApJ*, 744, L9
- Mashchenko, S., Couchman, H. M. P., & Wadsley, J. 2006, *Nature*, 442, 539
- Mashchenko, S., Wadsley, J., & Couchman, H. M. P. 2008, *Science*, 319, 174
- Mateo, M. L. 1998, *ARA&A*, 36, 435
- McConnachie, A. W. 2012, *AJ*, 144, 4
- Miller, B. W. *Globular Clusters in Dwarf Galaxies*, ed. Richtler, T. & Larsen, S., 141
- Navarro, J. F., Eke, V. R., & Frenk, C. S. 1996, *MNRAS*, 283, L72
- Navarro, J. F., Frenk, C. S., & White, S. D. M. 1995, *MNRAS*, 275, 720
- Oh, S.-H., de Blok, W. J. G., Brinks, E., Walter, F., & Kennicutt, Jr., R. C. 2011, *AJ*, 141, 193
- Pontzen, A. & Governato, F. 2012, *MNRAS*, 421, 3464

- Robertson, B., Bullock, J. S., Font, A. S., Johnston, K. V., & Hernquist, L. 2005, *ApJ*, 632, 872
- Searle, L. & Zinn, R. 1978, *ApJ*, 225, 357
- Stadel, J., Potter, D., Moore, B., et al. 2009, *MNRAS*, 398, L21
- Stinson, G. S., Dalcanton, J. J., Quinn, T., Kaufmann, T., & Wadsley, J. 2007, *ApJ*, 667, 170
- Zinn, R. 1980, *ApJ*, 241, 602
- Zolotov, A., Willman, B., Brooks, A. M., et al. 2010, *ApJ*, 721, 738